Closed-loop miscibility gap in sulfur–tellurium melts: structural evidence and thermodynamic modelling

2006 J. Phys.: Condens. Matter 18 11471

(http://iopscience.iop.org/0953-8984/18/50/005)

INSTITUTE OF PHYSICS PUBLISHING JOURNAL OF PHYSICS: CONDENSED MATTER

J. Phys.: Condens. Matter **18** (2006) 11471–11486 doi:10.1088/0953-8984/18/50/005

Closed-loop miscibility gap in sulfur–tellurium melts: structural evidence and thermodynamic modelling

Marie-Vanessa Coulet[1], **Robert Bellissent**[2] **and Christophe Bichara**[3]

[1] Laboratoire TECSEN, CNRS-Université Paul Cézanne, Campus de St Jérôme, Case 251, 13397 Marseille Cedex 20, France
[2] European Synchrotron Radiation Facility, BP 220, 38043 Grenoble Cedex, France
[3] Centre de Recherches en Matière Condensée et Nanosciences—CNRS, Campus de Luminy, Case 913, 13288 Marseille, France

E-mail: vanessa.coulet@univ-cezanne.fr

Received 27 July 2006, in final form 18 October 2006
Published 27 November 2006
Online at stacks.iop.org/JPhysCM/18/11471

Abstract

This paper concerns the existence of a closed-loop miscibility gap in sulfur–tellurium liquid alloys for a concentration of 40 at.% sulfur. We first present direct structural evidence of this two-phase domain based on neutron scattering measurements. In the second part, the driving mechanisms leading to this phase separation are discussed. A structural analysis combined with thermodynamic modelling shows that the existence of this closed-loop miscibility gap is strongly related to the structural changes occurring in pure liquid tellurium.

(Some figures in this article are in colour only in the electronic version)

1. Introduction

In past years the existence of liquid–liquid phase separation has triggered a large amount of experimental and theoretical work to elucidate the underlying mechanisms of this peculiar behaviour of liquid matter. Theoretical studies based on a hard sphere model have identified the size and packing fraction of the different species as the origin of a phase separation. These works [1] have shown that binary mixtures of hard spheres with a size ratio in the range from 0.05 to 0.20 exhibit a demixing transition in the liquid state. The fact that such small size ratios are not present in a number of inorganic binary systems which show a liquid–liquid phase separation [2] indicates that, beside geometrical considerations, bonding properties also have to be taken into account for a proper understanding. In covalent systems the effect of chemical bonding even becomes predominant because of its directional character. In these systems the phase separation is assumed to be a manifestation of subtle changes in the balance between the competing bonding trends of the different elements. This can be exemplified by many binary mixtures containing at least one element with a directional bonding character, such as, for instance, AgTe, FeTe, etc. Such alloys often show one or two miscibility gaps in their

phase diagrams [3]. However, the separation between size and bonding effects is somewhat artificial, because they are intimately related to the bond length, which is clearly dependent on its coordination number. It remains that, except for systems where significant changes of the electronic structure are observed, the atomic size of an element does not change significantly upon melting, whereas the characteristics of the bonding may change more drastically if it undergoes a structural change in the liquid state.

In some systems, generally organic solutions where the hydrogen bonding plays a fundamental role, a closed region describing liquid–liquid immiscibility is observed in the phase diagram. Such a closed-loop miscibility gap (CLMG) was first reported in the water–nicotine system [4] and in aqueous solutions of butan-2-ol [5]. This behaviour is also found in many other systems, such as alkypiridine solutions [6], polymer solutions [7, 8] etc. To our knowledge, the sulfur–tellurium phase diagram stands as a unique example of a binary inorganic system presenting re-entrant liquid–liquid miscibility. The experimental facts supporting this peculiar behaviour are, up to now, of indirect nature. Firstly, density measurements performed by γ-ray attenuation in the liquid state led to the conclusion that a two-phase domain exists in a narrow temperature range (953 K $< T <$ 993 K) and concentration range ($0.36 < x_s < 0.42$) [9]. Secondly, anomalies were also observed in the temperature evolution of the sound velocity [10] and in the conductivity [11]. This unusual behaviour could be related to the complex structural behaviour of liquid tellurium. It is well established that tellurium undergoes a structural change in the (undercooled) liquid state, evidenced by a well-defined maximum of the thermodynamic response functions such as specific heat, magnetic susceptibility and isothermal compressibility [12–14]. Neutron scattering [15] and x-ray absorption [16] measurements, complemented by computer simulations [17], have shown that the number of first neighbours in liquid tellurium increases from two in the low-temperature state up to a value closer to three in the high-temperature regime. This structural change takes place at around 693 K and is related to a covalent enhancement of the interchain bonds. The temperature at which this structural change takes place is shifted to higher values by adding sulfur or selenium, because the effect of adding one of these elements is to reduce the formation of such interchain bonds [18–20]. As a result of these competing effects, selenium-as well as sulfur-based tellurium alloys display complex thermodynamic behaviour in the liquid state [37]. At low temperatures, the enthalpy of mixing of the Se–Te system is negative, corresponding to an ordering tendency, while it becomes positive in the Te-rich side at higher temperatures, indicating a tendency for phase separation. A statistical model, based on the regular solution model and allowing the coordination of the elements to vary, could provide some insight into the mechanisms responsible for this tendency [21]. However, this effect is not strong enough to give rise to a miscibility gap, as in the case of S–Te system.

The present work is devoted to a structural and thermodynamic study of S–Te liquid alloys. The motivation for performing neutron scattering experiments on this system is two fold. Firstly, there is no direct evidence of the existence of the CLMG. Small-angle scattering measurements performed at a concentration inside the miscibility gap ($x_s = 0.4$) allowed us to observe and quantify the onset and the increase of concentration fluctuations in the liquid. In a similar way, the total structure factors of the two phases in equilibrium were measured, and they showed that two different liquids co-exist. Secondly, the driving mechanisms leading to this phase separation are analysed. A detailed study of the local order in the liquid state is presented over a large concentration and temperature range. The whole set of measured total structure factors is analysed using structural modelling in order to obtain total and partial coordination numbers. Combined with the statistical model cited above, a possible scenario for the mechanisms involved in the phase separation is proposed.

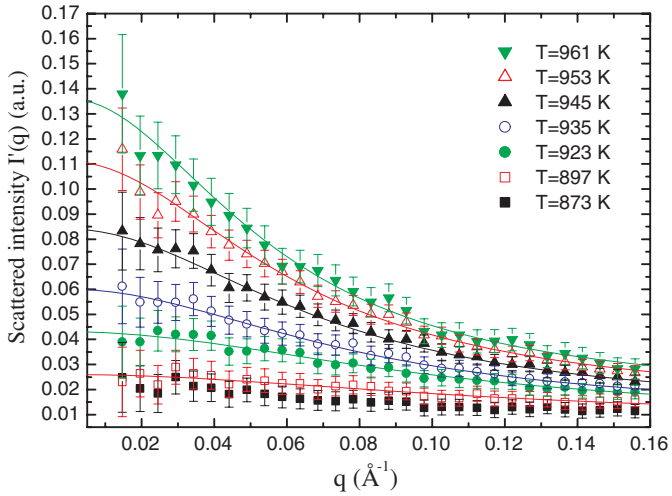

Figure 1. Small-angle scattered intensities for a $S_{0.4}Te_{0.6}$ alloy at different temperatures. Items are experimental data and the solid lines represent the fitted curves determined using the Ornstein–Zernike formalism [24].

2. Experiment

The samples were prepared by direct alloying of the pure elements (sulfur 99.9995% and tellurium 99.9999% from Alfa-Johnson Mattey). The elements were introduced as small pieces in silica containers and sealed under vacuum. All the samples were slowly heated up to the liquid state to ensure the homogeneity of the starting melt. This procedure was performed *in situ* by using a vanadium resistor. The temperature was measured using a K-type thermocouple within an accuracy of 5 K. The geometry of the silica containers depends on the experiment: silica tubes (inner diameter 10 mm, outer diameter 12 mm) were used to perform local order measurements, while a flat cylindrical quartz vessel (diameter 25 mm, height 10 mm, wall thickness 1 mm) was used for small-angle neutron scattering experiments (SANS).

Local order measurements were performed on the 7C2 two-axis diffractometer of the Orphee reactor at the Laboratoire Leon Brillouin (Saclay, France). The chosen wavelength was equal to 0.707 Å using the Cu(111) Bragg reflection. The diffraction spectra were recorded with a 640-cell multidetector, which provides an accurate determination of the structure factor over a momentum transfer range q between 0.3 and 16 Å^{-1} [22].

Small-angle neutron scattering experiments were performed at the same reactor on the PACE spectrometer. In order to be able to detect concentration fluctuations, we chose an incident wavelength equal to 5 Å, which allowed us to cover a q range between 0.0156 and 0.156 Å^{-1} in the present experimental set-up.

3. Structural evidence for a phase separation

3.1. Small-angle neutron scattering

Figure 1 presents the obtained small-angle scattered intensities for a $S_{0.4}Te_{0.6}$ alloy at different temperatures. Standard procedures were applied to subtract the contribution of the empty cell [23].

At 773 and 873 K, the signal is flat, which is characteristic of an homogeneous liquid. As the temperature is raised the signal increases, revealing the development of long-range

correlation in the liquid caused by concentration fluctuations. The high vapour pressure (mainly due to sulfur) turned out to be a major problem. Due to the explosion of the cell during the experiment, the maximum temperature that could be reached was 961 K. However the number of measured points is sufficient to conclude that the onset of concentration fluctuation is a signature of the presence of liquid–liquid phase separation.

In order to analyse these inhomogeneities, it is necessary to relate the structure factor for low q values to the concentration fluctuations of the system. In the case of a binary mixture, it is convenient to use the Bhatia–Thornton partials [25]. Within this formalism, the total structure factor is obtained as a linear combination of three partial structure factors, S_{NN}, S_{NC}, and S_{CC}, which explicitly introduce the concept of concentration correlation (the subscripts N and C refer to density and concentration correlations, respectively):

$$S(q) = \frac{\langle b\rangle^2}{\langle b^2\rangle} S_{NN}(q) + \frac{2\Delta b}{\langle b^2\rangle} S_{NC}(q) + \frac{\Delta b^2}{\langle b^2\rangle} S_{CC}(q) \tag{1}$$

with $\langle b\rangle = x b_S + (1-x) b_{Te}$, $\langle b^2\rangle = x b_S^2 + (1-x) b_{Te}^2$ and $\Delta b = b_{Te} - b_S$. b_S and b_{Te} are, respectively, the coherent scattering lengths of sulfur and tellurium, and x is the atomic fraction fraction of sulfur.

At $q = 0$, and following Bhatia and Thornton [25], the three partial terms became a simple expression of macroscopic quantities:

$$S_{NN}(0) = \frac{N}{V} k_B T \beta_T + \delta^2 S_{CC}(0) \tag{2}$$

$$S_{NC}(0) = -\delta S_{CC}(0) \tag{3}$$

$$S_{CC}(0) = N k_B T \frac{1}{(\frac{\delta^2 G}{\delta^2 x^2})_{T,P,N}} \tag{4}$$

with

$$\delta = \frac{N}{V}(V_{Te} - V_S) \tag{5}$$

where k_B is the Boltzman constant, G is the free enthalpy, V_S and V_{Te} are the partial molar volumes, and β_T is the isothermal compressibility.

Using the above equations, the null-angle total structure factor can then be written:

$$S(0) = A\beta_T + B S_{CC}(0) \tag{6}$$

with

$$A = \frac{\langle b\rangle^2}{\langle b^2\rangle} \frac{N}{V} k_B T \tag{7}$$

$$B = \left(\frac{N}{V}\right)^2 \frac{(V_{Te} b_S - V_S b_{Te})^2}{\langle b^2\rangle}. \tag{8}$$

For a binary liquid alloy, the compressibility and the partial volume are slowly varying functions of temperature, compared to the strong divergence of the term $(\frac{\delta^2 G}{\delta^2 x_S^2})^{-1}$ or $S_{CC}(0)$ approaching the critical point. Therefore, the strong divergence of the concentration fluctuations will dominate the small-angle scattering near the critical point [26].

In order to analyse the small-angle pattern, it is conventional to use the Ornstein–Zernike formalism [24]. Recently this formalism allowed us to evidence density fluctuations above the critical point in supercritical selenium [27]. According to this theory and using the description of Bhatia and Thornton, the structure factor is a Lorentzian function of the diffusion vector q:[4]

$$S(q) = 1 + \frac{A\beta_T + B S_{CC}(0) - 1}{1 + q^2\xi^2}. \tag{9}$$

[4] For the details of the calculation, please see [26].

Table 1. Values of the parameters resulting from the fitting procedure using Ornstein–Zernike formalism.

T (K)	I_0 (a.u.)	A' (a.u.)	ξ (Å)
897	0.008 ± 0.003	0.018 ± 0.003	8.57 ± 1.98
923	0.008 ± 0.003	0.035 ± 0.002	9.79 ± 1.04
935	0.010 ± 0.001	0.050 ± 0.001	12.52 ± 0.63
945	0.011 ± 0.001	0.073 ± 0.001	14.00 ± 0.51
953	0.013 ± 0.002	0.097 ± 0.002	15.79 ± 0.81
961	0.016 ± 0.002	0.118 ± 0.002	17.52 ± 0.88

The SANS experiment did not provide the structure factor $S(q)$ directly, but an intensity $I_{\text{meas}}(q)$ related to $S(q)$ by the relation:

$$I_{\text{meas}}(q) = I_0 S(q) + I_{\text{B}}(q) \tag{10}$$

where I_0 is a normalization factor depending in the neutron flux and the scattering power of the sample. $I_{\text{B}}(q)$ is a background which includes the scattering from the vessel and the quartz cell, as well as the incoherent contribution of the sample and the multiple scattering effects. The determination of $I_{\text{B}}(q)$ is not simple and it is usual to take a sample run performed at temperatures far from the critical region as $I_{\text{B}}(q)$. For this thermodynamic state, the value $S_{\text{CC}}(0)$ and the correlation length ξ are negligibly small [26].

We used the sample run at 773 K to determine $I_{\text{B}}(q)$, and hence we have:

$$I_0 S(q) = I_{\text{meas}}(q) - I_{773}(q) = I'(q). \tag{11}$$

Using equation (9), we obtain:

$$I'(q) = I_0 + \frac{(A\beta_T - 1)I_0 + B S_{\text{CC}}(0) I_0}{1 + q^2\xi^2}. \tag{12}$$

At a fixed temperature, the quantity $(A\beta_T - 1)I_0 + B S_{\text{CC}}(0)$ is assumed to be a constant, so we fitted our data for each temperature using the following equation:

$$I'(q) = I_0 + \frac{A'}{1 + q^2\xi^2}. \tag{13}$$

The fitted curves, obtained using a standard nonlinear least-square regression method, are represented by solid lines in figure 1. The values obtained for I_0, A' and ξ are listed in table 1. As there are no data available for the partial volumes and the isothermal compressibility in the temperature range considered here, we could not deduce the absolute values of $S_{\text{CC}}(0)$.

An estimate of the value of the lower critical temperature can be obtained by fitting the obtained values of ξ (Å) according to mean field theory. In this approximation, the correlation length is written as:

$$\xi = \xi_0 \left(\frac{T - T_{\text{c}}}{T_{\text{c}}} \right)^{-\nu} \tag{14}$$

with $\nu = 0.5$.

The fit of the values of ξ, presented in figure 2, is satisfactory and leads to a value for the critical temperature equal to 983 K $\pm$ 20 K. The value published by Tsuchiya [11] (953 K) is slightly lower, but within the accuracy that we can expect from our rather indirect determination.

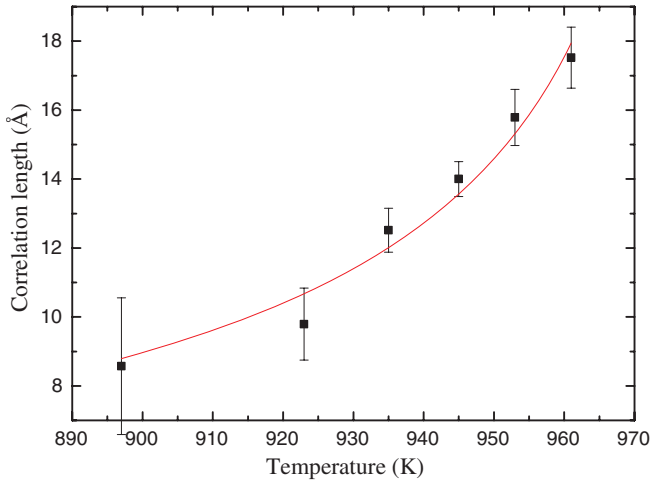

Figure 2. Evolution of the correlation length with increasing temperature. Items are the obtained values using the Ornstein–Zernike formalism, and the solid line results from a fitting of these data in the mean-field approximation.

3.2. Local order of the two phases in equilibrium

The method used to perform local order measurements of the two phases in equilibrium has been described previously in [28]. The sample, inside its container, is regularly turned upside-down during the experiment in order to avoid unwanted concentration gradients. In addition, an automatically driven diaphragm enables us to measure separately the lower and the upper part of the sample, which respectively correspond to more dense and the less dense phases in equilibrium.

Figure 3 presents the measured structure factors at three different temperatures. On each panel, the structure factor measured in the bottom and in the top of the container are represented as well as the difference signal. The time evolution of the signal was checked by alternating small counting sequences on the top and bottom parts.

For each measurement, the structure factor was obtained by subtracting from the total signal the contribution of all the elements passing in the beam in exactly the same geometry. The Paalman and Pings method [29] was used to obtain the transmission factor, providing that both transmission and absorption processes are taken into account. Inelastic effects were corrected using the method proposed by Placzek [30] and a standard multiple scattering correction [31] was applied. An absolute normalization was performed using the scattered intensity from a vanadium sample with a geometry identical to that of the samples.

As shown by the difference plot, at a temperature below the miscibility gap ($T = 773$ K) (figure 3(a)), the two structure factors are the same within the statistical accuracy. At 993 K (figure 3(b)), differences between the two structure factors can be noticed, essentially located at low q values: in the upper part of the tube, the structure factor presents a shoulder at around 1.5 Å^{-1}, and the first peak at around 2 Å^{-1} is less intense than the second. As shown by our previous work [32], these features are characteristic for a sulfur-rich phase. The difference plot displays oscillations up to 8 Å^{-1} and is smeared out at high q values. This point will be discussed in detail in the next section. At higher temperature (1053 K), the two structure factors became identical (figure 3(c)), the system is homogeneous again.

We must point out that the difference observed between the two structure factors is small. However we are convinced that it is significant for structural changes, as the statistical noise is

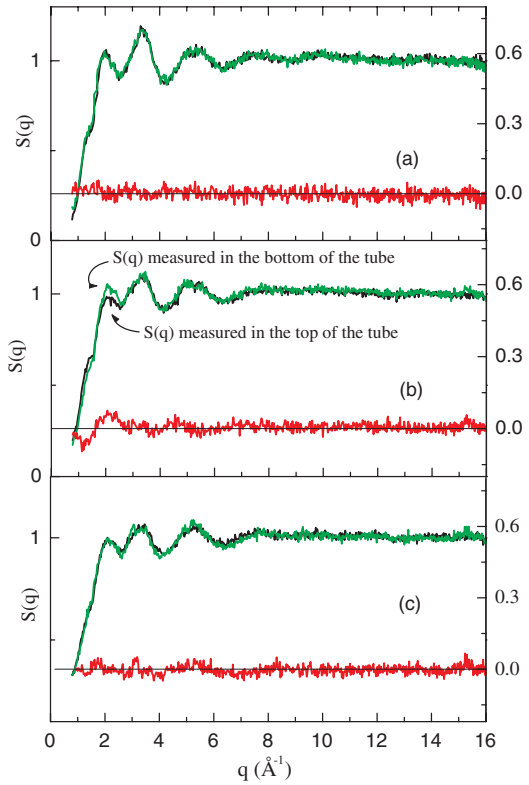

Figure 3. Structure factors measured in the lower (grey (green)) and upper (black) part of the tube at $T = 773$ K (a), $T = 993$ K (b) and $T = 1053$ K (c). In the bottom part of the graph the difference between the two signals is represented.

clearly inferior to the amplitude of the oscillations. Moreover, to make sure that any difference between the two measurements is not an artefact, the measurements in the bottom and in the top were performed with short time intervals before summing up to improve the signal-to-noise ration. Several measurements performed at the same temperatures show the same result.

4. Driving mechanisms for the phase separation

4.1. Neutron scattering study combined with a structural model

The measured structure factors of S_xTe_{1-x} liquid alloys ($x = 0.1$, 0.2, 0.3, 0.4, 0.5, 0.6 and 0.8) are presented in figures 4–6 at 723, 873 and 1023 K, respectively. Some of these data have already been published in [32]. Here we present a more complete study over the whole concentration range. The same corrections, as described in the previous section, were applied to the raw data in order to obtain the structure factors.

The principle of modelling the structure factor at high q value was first used to describe the molecular geometry in fullerene C_{60} powders [33]. We propose a generalization of this method suitable to a chain network. This extension of the model is reasonable as, in the present system, first neighbours are strongly bonded with directional covalent bonds, whereas neighbours at higher distances are weakly bonded and do not contribute much to the structure factor in the large q range.

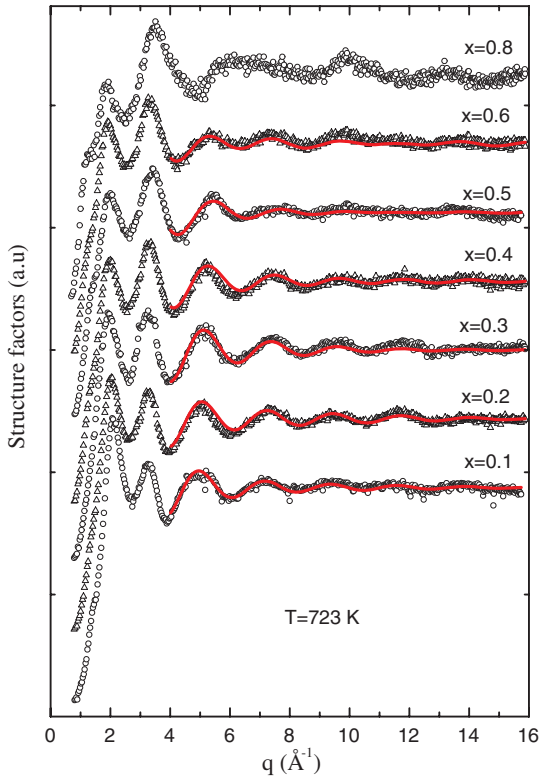

Figure 4. Experimental (symbols) and modelled (solid lines) total structure factors of S_xTe_{1-x} liquid alloys at 723 K. The curves were shifted in order to ensure legibility.

The modelling procedure [32] consists of writing the structure factor as:

$$S(q) = \frac{x_S^2 b_S^2}{\langle b\rangle^2} S_{SS}(q) + \frac{x_{Te}^2 b_{Te}^2}{\langle b\rangle^2} S_{TeTe}(q) + 2\frac{x_S x_{Te} b_S b_{Te}}{\langle b\rangle^2} S_{STe}(q) \tag{15}$$

where S_{SS}, S_{TeTe} and S_{STe} are the partial structure factors corresponding to sulfur–sulfur, tellurium–tellurium and sulfur–tellurium contributions, respectively. b_{Te} and b_S are the scattering lengths of tellurium and sulfur and $\langle b\rangle = (x_{Te}b_{Te} + x_S b_S)$. We approximate the partial structure factors $S_{ij}(q)$ at large q values by retaining only one distance (r_{ij}), typically the first-neighbour distance between species i and j:

$$S_{ij}(q) = \frac{N_{ij}}{x_j}\frac{\sin(qr_{ij})}{qr_{ij}}\exp\left(\frac{-q^2\langle u_{ij}\rangle^2}{2}\right) \tag{16}$$

where i or j are either S or Te, u_{ij} characterizes the fluctuations of the bond distances r_{ij}, and N_{ij} is the average number of atoms j surrounding atom i.

In addition, by taking into account the structural changes undergone by pure liquid tellurium [15, 17], the partial structure factor of tellurium $S_{TeTe}(q)$ is assumed to be the sum of intrachain and interchain contributions. This is writen:

$$S_{TeTe}(q) = S_{TeTe_S}(q) + S_{TeTe_L}(q) \tag{17}$$

where S_{TeTe_S} corresponds to the contribution of the intrachain distance (short TeTe distance $r_{TeTe_S} \sim 2.8$ Å) and $S_{TeTe_L}(q)$ corresponds to the interchain distance (long TeTe distance: $r_{TeTe_L} \sim 3.15$ Å).

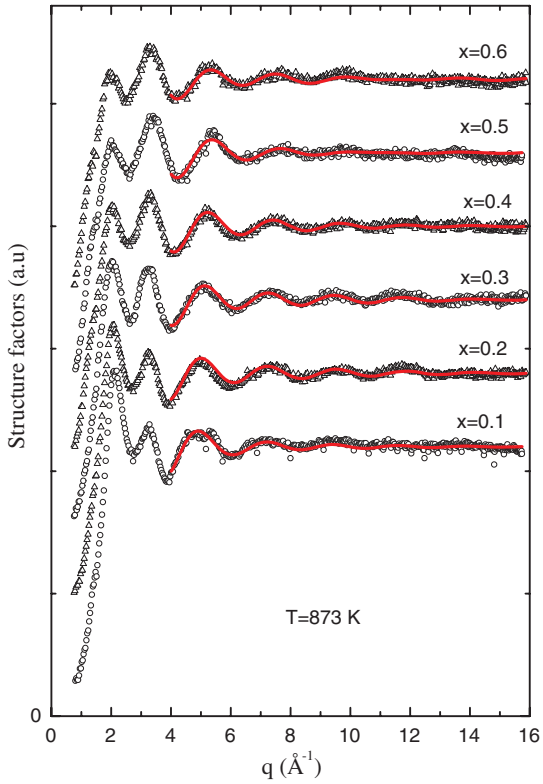

Figure 5. Experimental (symbols) and modelled (solid lines) total structure factors of S_xTe_{1-x} liquid alloys at 873 K. The curves were shifted in order to ensure legibility.

The structure factors modelled are represented by solids lines on figures 4–6. As seen in equation (16), this approximation is restricted to q values larger than ∼4 Å^{-1}. The term accounting for the disorder $\exp(\frac{-q^2\langle u_{ij}\rangle^2}{2})$ (Debye–Waller factor) for the distances S–S, S–Te, $TeTe_L$ and $TeTe_S$ is plotted in figure 7. One can see that these contributions are strongly damped beyond ∼16 Å^{-1}. However, the Debye–Waller factor associated with the $TeTe_L$ distance decays much faster than the others. This supports the approximation of considering only four distances in the model, since the contributions of longer distances will be strongly smeared out.

This modelling procedure yields the partial and total coordination numbers, plotted in figures 8 and 9 respectively, over wide concentration and temperature ranges. The partial coordination numbers of sulfur and tellurium are defined as $N_{Te} = N_{TeTe} + N_{TeS}$ and $N_S = N_{SS} + N_{STe}$, respectively, and the total coordination number is defined as $N = (1-x)N_{Te} + xN_S$. The results can be summarized as follows. Firstly, the total coordination number is higher on the tellurium-rich side and increases with temperature. This is in agreement with the published results for the structure of pure liquid sulfur which has two first neighbours over the whole temperature range [34] and pure liquid tellurium whose number of nearest neighbours increases from ∼2.3 (at the melting point) up to 3 [15, 17]. Secondly, at 723 K, the variation in the total coordination number is weak (from 2.3 down to 2.0). This is related to the small amount of three-fold coordinated Te atoms at low temperature. For higher temperatures, the total coordination number rapidly decreases in the concentration range between $x = 0.1$ and 0.4 and the decrease is sharper as the temperature is increased. This variation in the total

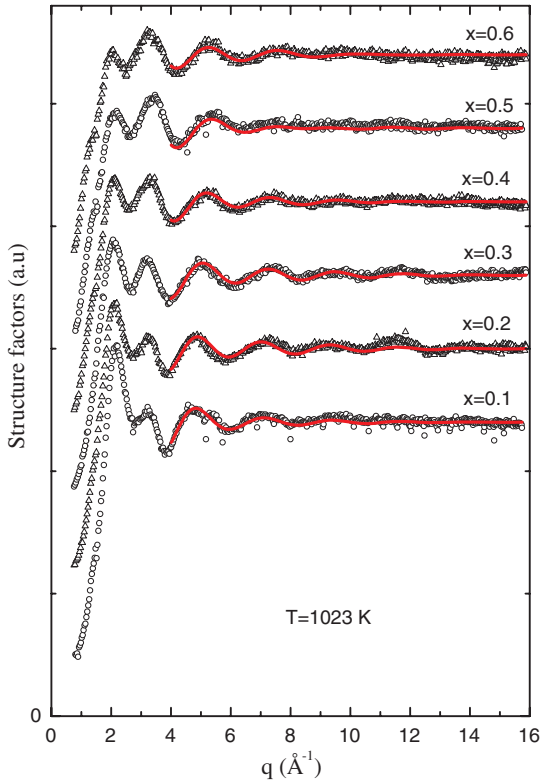

Figure 6. Experimental (symbols) and modelled (solid lines) total structure factors of S_xTe_{1-x} liquid alloys at 1023 K. The curves were shifted in order to ensure legibility.

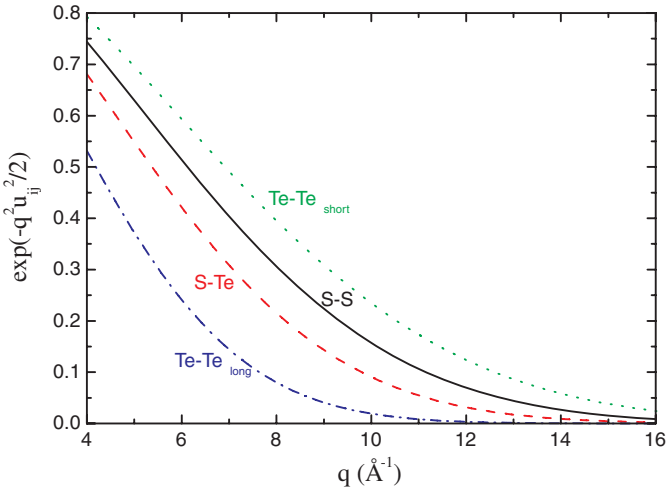

Figure 7. Debye–Waller factors associated to the S–S (line), S–Te (dashed line), Te–Te_c (dotted line) and Te–Te_c (dashed-dotted line) distances. The u_{ij} values used correspond to the $S_{0.3}Te_{0.7}$ alloy at 1023 K.

coordination number is essentially related to the partial coordination of Te, which increases because interchain Te–Te bonds are formed (figure 8).

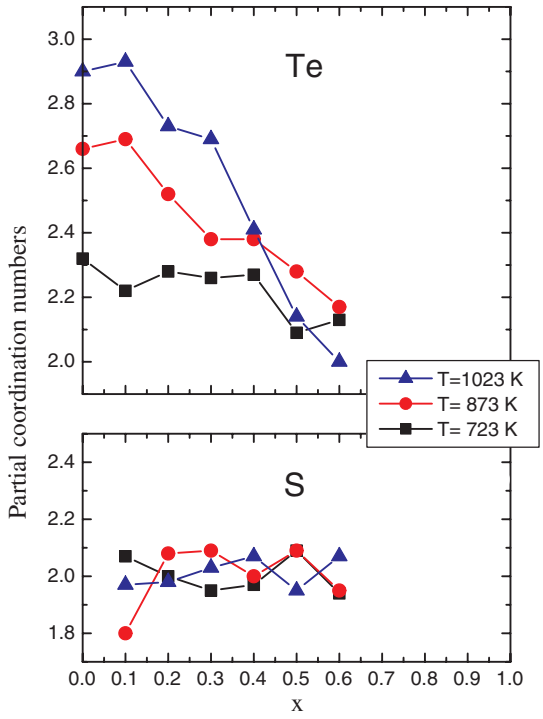

Figure 8. Evolution of the partial coordination number of tellurium and sulfur as a function of the sulfur concentration x, at three temperatures.

At this point, we can explain more precisely the difference between the structure factors measured on both sides of the miscibility gap (see section 3.2). Since the Debye–Waller factor associated with the Te–Te interchain distances decays rapidly and since the structure of the two liquids in equilibrium essentially differs by the number of $TeTe_L$ distances, the changes in the structure factors of figure 3 are noticeable only in the small-q region.

4.2. Thermodynamic modelling

We propose to relate the mixing thermodynamic quantities of the binary system S–Te and the coordination number obtained from the neutron scattering experiments. To this aim, we use a regular model with multiple connectivity, as developed by Amzil *et al* [21] for the parent Se–Te system. This model is based on the regular solution model developed by Guggenheim [35] with three supplementary hypotheses:

- the binary alloy is treated as a ternary system with S, Te^{II} and Te^{III} atoms, with coordination numbers equal to 2, 2 and 3, respectively;
- contrary to a classical regular solution model, the lattice does not have a constant coordination number—it depends on the nature of the atoms and on the temperature;
- the equilibrium $Te^{II} \rightarrow Te^{III}$ in the presence of sulfur is described explicitly in terms of pairs interactions.

The calculation of the configurational partition function and of the thermodynamics functions is done within the Bragg–William statistical treatment (zero-order approximation) which assumes a random distribution of the species on the network [36]. The details of the

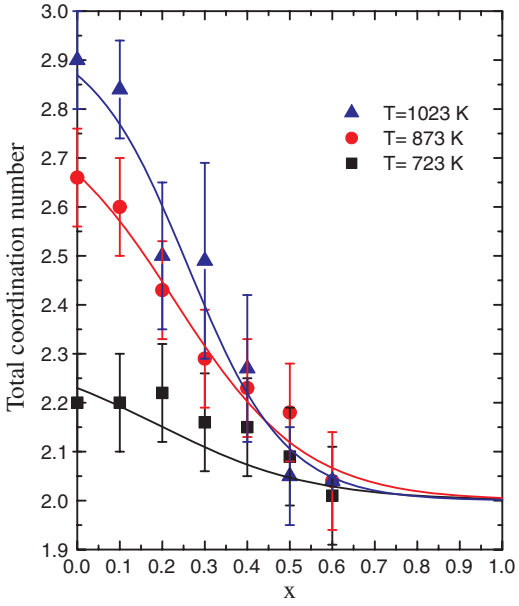

Figure 9. Evolution of the number of nearest neighbours as a function of the sulfur concentration x, at three temperatures. The line is the interpolation used for thermodynamic modelling (see text in section 4.2).

calculation are given in [21]; here, we just remind us of the main results. The Gibbs energy of mixing is written as:

$$\Delta G^m = [x_3 - (1 - X_{23})(1 - x)]\Delta G^0 + \frac{2xx_2}{d}W_{12} + \frac{3xx_3}{d}W_{13} + \left[\frac{3x_2x_3}{d} - (1 - x)\frac{6X_{23}(1 - X_{23})}{3 - X_{23}}\right]W_{23} + RT[x\ln x + x_2\ln x_2 + x_3\ln x_3 - (1 - x)\{X_{23}\ln X_{23} + (1 - X_{23})\ln(1 - X_{23})\}] \quad (18)$$

where

- x, x_2, x_3 are the molar fraction in the melt of S, Te^{II} and Te^{III} respectively;
- X_{23} is the molar fraction of Te^{II} upon the total number of tellurium atoms ($Te^{II} + Te^{III}$) in pure tellurium;
- d is defined as $d = x + x_2 + \frac{3}{2}x_3$,
- W_{12}, W_{13} and W_{23} are interchange energies corresponding to the pairs S–Te^{II}, S–Te^{III} and Te^{II}–Te^{III};
- ΔG^0 is the standard Gibbs energy of the transformation reaction $Te^{II} \Leftrightarrow Te^{III}$.

The enthalpy of mixing ΔH^m derives from ΔG^m:

$$\Delta H^m = [x_3 - (1 - X_{23})(1 - x)]\Delta H^0 + \frac{2xx_2}{d}W_{12} + \frac{3xx_3}{d}W_{13} + \left[\frac{3x_2x_3}{d} - (1 - x)\frac{6X_{23}(1 - X_{23})}{3 - X_{23}}\right]W_{23} \quad (19)$$

and the entropy of mixing ΔS^m is written:

$$\Delta S^m = R[x\ln x + x_2\ln x_2 + x_3\ln x_3 - (1 - x)\{X_{23}\ln X_{23} + (1 - X_{23})\ln(1 - X_{23})\}]. \quad (20)$$

Table 2. Values of the parameters a_0, a_1 and a_2.

T (K)	a_0	a_1	a_2
723	0.31	0.19	0.18
873	0.815	0.23	0.153
1023	0.96	0.26	0.115

The equilibrium condition between tellurium atoms Te^{II} and Te^{III} can be written:

$$RT \ln \frac{X_{23}}{1 - X_{23}} = \Delta G^0 - 6\left(1 - \frac{6}{(3 - X_{23})^2}\right) W_{23}. \tag{21}$$

The thermodynamic quantities ΔG^m, ΔH^m and ΔS^m formally depend on six parameters, which are the interchange energies W_{12}, W_{13} and W_{23} and the molar fraction of sulfur (x), $Te^{II}(x_2)$ and $Te^{III}(x_3)$.

The total coordination number N can be written as a function of the concentration of the different species in the system, i.e. $N = 2x + 2x_2 + 3x_3$. Bearing in mind that we have $x + x_2 + x_3 = 1$, we are able to express N only as a function of x. This means that, at a given sulfur concentration, the thermodynamic quantities only depend on the interchange energies and on the total coordination number. We therefore express the concentration dependence of the total coordination number resulting from the previous structural modelling in the form:

$$N(x) = 2 + \frac{a_0}{1 + \exp\left(\frac{x - a_1}{a_2}\right)}. \tag{22}$$

Table 2 gives the adopted values for a_0, a_1 and a_2 at the three temperatures 723, 873 and 1023 K, and the continuous lines on figure 9 show the result obtained.

In the work of Amzil *et al* [21], the experimental enthalpy of mixing was used to fit the parameter of the model, and the coordination number was deduced from the thermodynamic quantities. Here, since we do not have any reliable thermodynamic data, we assume that W_{23} (Te^{II}–Te^{III} interaction) has the same value as in the parent Se–Te system, i.e. $W_{23} = 5$ kJ mol^{-1}. Moreover, as the phase diagram of the S–Te system displays a large eutectic, it seems reasonable to choose positive values for W_{12} and W_{13}. The order of magnitude of the enthalpy of mixing [37] and the variation of the specific heat as a function of x and T [38] lead us to propose $W_{12} = 6$ kJ mol^{-1} and $W_{13} = 8$ kJ mol^{-1}. We checked the stability of our results by varying the W_{ij} values in a reasonable interval around the above values. For too large absolute values, the enthalpy is systematically higher than the entropy and this leads, for the temperatures of interest, either to a homogeneous liquid $W_{ij} < 0$ or to a demixing liquid $W_{ij} > 0$. Let us note that, in the Bragg–Williams approximation used here, the entropy is only a function of x, x_2, x_3 and X_{12} and these values are fixed with the results we obtain from the structural modelling of the neutron scattering data. The W_{ij} values only modulate the amplitude of the contribution of the enthalpy to ΔG^m.

The thermodynamic quantities obtained within this approximation are represented in figures 10–12. They were calculated at 723, 873 and 1023 K and also in the high temperature limit. In this limiting case, we assume that the equilibrium Te^{II}–Te^{III} is completely shifted towards the Te^{III} species. This correspond to $X_{12} = 0$ and $x_2 = 0$ in equations (18), (19) and (20); that is to say, to a binary solution of S and Te^{III}. The coordination number varies linearly from three down to two, and we obtain an ideal entropy of mixing for a classical binary system.

The behaviour of the Gibbs energy of mixing (figrue 10) indicates that the liquid is homogeneous at 723 K and at 873 K, and that a phase separation occurs at 1023 K. Obviously,

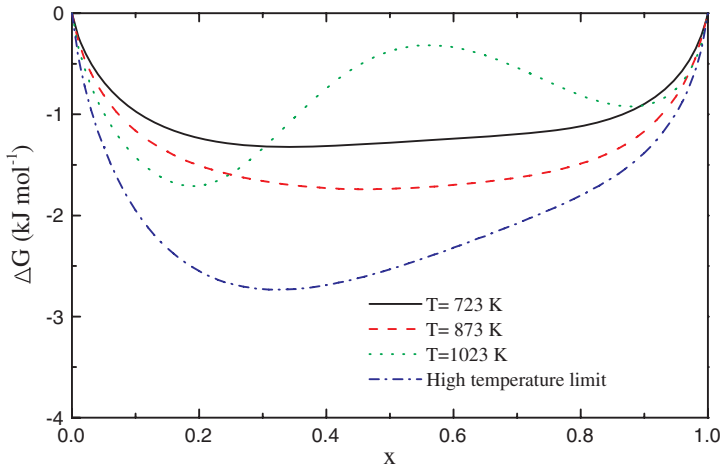

Figure 10. Variation in the Gibbs energy of mixing (free enthalpy) as a function of the concentration of sulfur (x) for different temperatures.

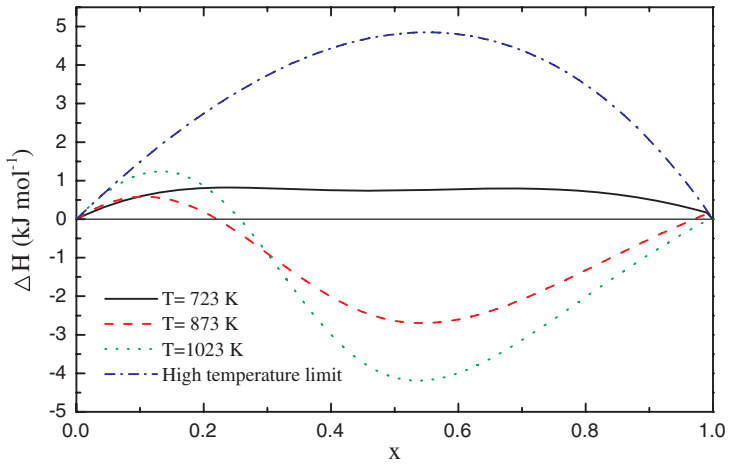

Figure 11. Variation in the enthalpy of mixing as a function of the concentration of sulfur (x) for different temperatures.

the two-phase domain is too broad in concentration and lies were at too high temperatures, but the model correctly yields a CLMG. Many reasons can account for the quantitative discrepancies. Firstly, we used an oversimplification of a lattice model to treat a complex sp bonding liquid. Secondly, the model is based on a disordered solution approximation [36] which neglects any order effect for the calculation of the thermodynamic quantities. At last, this model completely neglects the PV term in the calculation of the free enthalpy and enthalpy.

Analyses of the enthalpy (figure 11) and the entropy (figure 12) contributions to the Gibbs energy are interesting. The enthalpy is positive at 723 K and becomes partially negative at 873 and 1023 K. This is in agreement with our estimated values of excess specific heat. For Te-rich concentrations, the enthalpy of mixing always increases with temperature, and this tendency is reversed for the highest sulfur concentration. The entropy of mixing also presents an unusual behaviour. At 873 and 1023 K, it is negative in a quite large concentration range. This negative

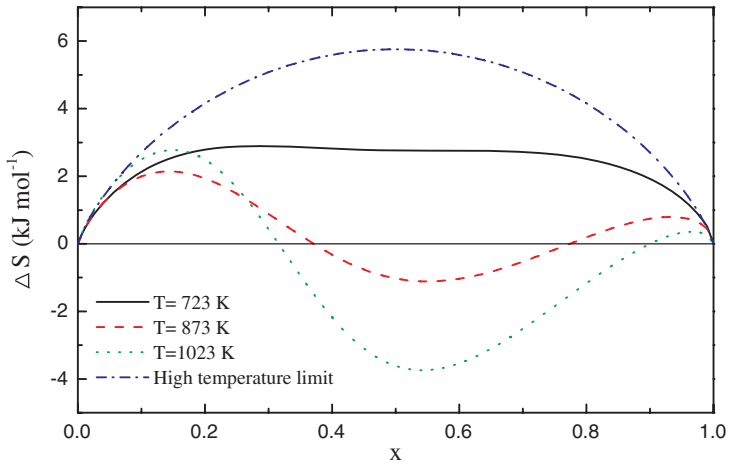

Figure 12. Variation in the entropy of mixing as a function of the concentration of sulfur (x) for different temperatures.

value of the entropy can be explained by remembering that the binary system is treated as a ternary one with a constraint on the molar fraction Te^{II} and Te^{III}.

Moreover, it has to be underlined that the nonlinear evolution of the total coordination number with the concentration—which indicates sharp structural changes in the melt—is a necessary condition for the miscibility gap to appear. Indeed, if we assume a linear dependance of the total coordination number $N(x) = 2+\alpha(1-x)$, this leads to an ideal entropy of mixing $\Delta S = R[x \ln x - (1-x)\ln(1-x)]$, which does not lead to any miscibility gap. This may explain why the CLMG is observed in the present system and not in Se–Te melts.

5. Conclusions

In the first part of this paper we gave a structural proof of the existence of a miscibility gap in the sulfur–tellurium system, as previously suggested by Tsuchiya [11]. Small-angle neutron scattering experiments indicate that the $S_{0.4}Te_{0.6}$ liquid is homogeneous just above the liquidus and that, with increasing temperature, concentration fluctuations develop when approaching the lower boundary of the CLMG. The structure factors of the two phases in equilibrium on both side of the CLMG were measured: small but significant differences are observed at low q values.

In the second part the partial coordination numbers obtained by fitting the total structure factors are used as an input for a statistical mechanical model, taking into account the peculiarities of this system (the change in the coordination number of the Te atoms). With some reasonable additional assumptions, the calculated thermodynamic quantities of mixing positively support the existence of a closed-looped miscibility gap. Although this second part is qualitative, it presents the major interest in providing a coherent interpretation of the complex thermodynamic and structural behaviour of this system. As in the parent Se–Te system, the dominant feature is the structural change undergone by Te atoms going from a coordination number of 2, forming chains in the undercooled regime, to about 3 at higher temperature. Adding sulfur shifts the crossover between these two states towards higher temperatures and, due to the positive (repulsive) interaction of the added sulfur atoms with the three-fold-coordinated tellurium atoms, a phase separation tendency develops. This tendency is stronger

in the S–Te system than in the parent Se–Te system and leads to phase separation at high temperature, although the low-temperature liquid (just above the liquidus) is homogeneous. At even higher temperatures, the larger contribution of the entropy of mixing makes the liquid homogeneous again.

References

[1] Biben T and Hansen J P 1991 *Phys. Rev. Lett.* **66** 2215
[2] Hansen M and Anderko K 1958 *Constitution of Binary Alloys* (New York: McGraw-Hill)
[3] Villars P, Prince A and Okamoto H 1995 *Handbook of Ternary Alloy Phase Diagram* (Materials Park, OH: ASM International)
[4] Hudson C S 1904 *Z. Phys. Chem.* **47** 113
[5] Dolgolenko W 1908 *Z. Phys. Chem.* **62** 499
[6] Andon R J L and Cox J D 1952 *J. Chem. Soc.* **1952** 4601
[7] Nord F F, Bier M and Timasheff S N 1951 *J. Am. Chem. Soc.* **73** 289
[8] Malcolm G N and Rowlinson J S 1957 *Trans. Faraday Soc.* **53** 921
[9] Tsuchiya Y 1990 *J. Non-Cryst. Solids* **117/118** 571
[10] Tsuchiya Y 1994 *J. Phys.: Condens. Matter* **6** 2451
[11] Tsuchiya Y 1992 *J. Phys.: Condens. Matter* **4** 4335
[12] Tsuchiya Y, Shibusawa S and Tamaki S 1977 *J. Phys. Soc. Japan* **42** 1578
[13] Tsuchiya Y and Seymour E F W 1985 *Solid State Phys.* **18** 4721
[14] Tsuchiya Y 1991 *J. Phys.: Condens. Matter* **3** 3163
[15] Menelle A, Bellissent R and Flank A M 1987 *Europhys. Lett.* **4** 705
[16] de Panfilis S and Filipponi A 1997 *Europhys. Lett.* **37** 397–402
[17] Bichara C, Raty J Y and Gaspard J P 1996 *Phys. Rev.* B **53** 206
[18] Tsuchiya Y 1988 *J. Phys. Soc. Japan* **57** 3851
[19] Tsuchiya Y 1991 *J. Phys. Soc. Japan* **60** 960
[20] Kakinuma F and Ohno S 1987 *J. Phys. Soc. Japan* **56** 619
[21] Amzil A, Gilbert M, Bichara C and Mathieu J C 1996 *J. Phys.: Condens. Matter* **8** 5281
[22] Ambroise J P and Bellisent R 1984 *Rev. Phys. Appl.* **18** 731
[23] Calmettes P 1999 *J. Physique Coll.* **9** 83
[24] Ornstein L S and Zernike F 1918 *Z. Phys.* **19** 134
[25] Bhatia A B and Thornton D E 1970 *Phys. Rev.* B **2** 3004
[26] Damay P, Leclercq F and Chieux P 1984 *J. Phys. Chem.* **88** 3734
[27] Coulet M V, Simonet V, Calzavara Y, Testemale D, Hazemann J L, Raoux D, Bley F and Simon J P 2003 *J. Chem. Phys.* **118** 11235
[28] Coulet M V, Céolin R, Bellissent R, Bergman C, Beuneu B, Ambroise J P and Bichara C 2002 *J. Non-Cryst. Solids* **312–314** 404
[29] Palmaan H H and Pings C J 1962 *J. Appl. Phys.* **33** 2635
[30] Placzek G 1952 *Phys. Rev.* **86** 377
[31] Blech I A and Averbach B L 1965 *Phys. Rev.* **137** A1113
[32] Coulet M V, Bellissent R, Bionducci M and Bichara C 1999 *Europhys. Lett.* **45** 175
[33] Damay P, Leclercq F and Chieux P 1989 *Phys. Rev.* B **40** 4696
[34] Bellissent R, Descotes L, Boué F and Pfeuty P 1990 *Phys. Rev.* B **41** 2135
[35] Guggenheim E A 1952 *Mixtures* (Oxford: Clarendon)
[36] Bragg W L and Williams E J 1934 *Proc. R. Soc.* A **151** 540
[37] Maekawa T, Yokokawa T and Niwa K 1973 *Bull. Chem. Soc. Japan* **46** 761
[38] Kakinuma F, Ohno S and Suzuki K 1993 *J. Non-Cryst. Solids* **156–158** 691